NACA

RESEARCH MEMORANDUM

THE EFFECT OF BASE BLEED ON THE BASE PRESSURE, LIFT,

DRAG, AND PITCHING MOMENT OF A 10-PERCENT-THICK

BLUNT-BASE AIRFOIL AT A MACH NUMBER OF 2.72

By Jim J. Jones

Langley Aeronautical Laboratory
Langley Field, Va.

NATIONAL ADVISORY COMMITTEE
FOR AERONAUTICS

NATIONAL ADVISORY COMMITTEE FOR AERONAUTICS

RESEARCH MEMORANDUM

THE EFFECT OF BASE BLEED ON THE BASE PRESSURE, LIFT,

DRAG, AND PITCHING MOMENT OF A 10-PERCENT-THICK

BLUNT-BASE AIRFOIL AT A MACH NUMBER OF 2.72

By Jim J. Jones

SUMMARY

An experimental investigation was made at a Mach number of 2.72 to measure the effect of base bleed on the base pressure, lift, drag, and pitching moment of a 10-percent-thick blunt-base airfoil model. On this model the base bleed was effected by bleeding air through small holes in the lower surface near the trailing edge into the base region. It was found that the zero-lift drag was reduced about 6 percent for the maximum value of the ratio of bleed-hole area to base area tested. Above a lift coefficient of about 0.075, an optimum value of this area ratio was found but the decrease in total drag at this optimum point over zero area (no base bleed) was very small. No boundary-layer-removal plates were used on the ends of the model; therefore, the model was not two dimensional in the sense that the side-wall boundary layer caused a spanwise pressure gradient. This spanwise pressure gradient was measured on the model at a station near the trailing edge.

INTRODUCTION

At high supersonic speeds the airfoil with minimum pressure drag for a given stiffness has a blunt trailing edge. (See, for example, ref. 1.) This condition arises from the fact that the drag contribution of the base is small at hypersonic speeds. Some bluntness might be beneficial at lower supersonic speeds if it were possible to increase efficiently the pressure acting on the base.

In reference 2 it was shown that the pressure on the base of a cone cyclinder could be raised by bleeding air through small noles on the cylindrical surface into the base region. The result was a decrease in total drag of the body since the decrease in base drag was larger than the drag increase due to the presence of the holes.

This so-called base-bleed principle was applied to a blunt-base air-foil in reference 3. In these tests the air to be introduced into the base region was not obtained from the main stream but rather from an external source. The tests showed the base pressure could be raised on a two-dimensional body by the same order of magnitude as on a body of revolution. However, these tests did not yield any data on the overall drag reduction since the penalties of the air-induction system were not included.

No complete analysis of the base-bleed mechanism has as yet been published. On bodies with blunt bases, the mixing zone which bounds the region of separated flow normally scavenges this separated region to a low pressure. It seems apparent from the tests of references 2 and 3 that the addition of only a small mass flow to the base region counterbalances this scavenging action so that the region is not evacuated to as low a pressure. These tests also indicated that the optimum stagnation pressure of the air to be exhausted out of the base is of about the same magnitude as the free-stream static pressure. The method of obtaining bleed air near the base of the model used in reference 2 has also been used in this investigation.

The purpose of the present investigation is to study the effectiveness of base bleed on an airfoil section by using a self-contained air-induction system. Base pressure, lift, total drag, and pitching moment were measured during the tests at a Mach number of 2.72.

SYMBOLS

A plan-form area of model

$\dfrac{A_H}{A_B}$ ratio of total area of holes to area of base

C_D drag coefficient, $\dfrac{\text{Drag}}{qA}$

C_L lift coefficient, $\dfrac{\text{Lift}}{qA}$

C_{L_α} lift-curve slope, $\dfrac{dC_L}{d\alpha}$

C_m pitching-moment coefficient about 67-percent station, $\dfrac{\text{Pitching moment}}{qAc}$

C_p local pressure coefficient, $\dfrac{p - p_\infty}{q}$

C_{p_B} base-pressure coefficient, $\dfrac{p_B - p_\infty}{q}$

c chord

M Mach number

p local static pressure

p_B base pressure

p_∞ free-stream static pressure

q free-stream dynamic pressure, $\dfrac{\gamma p_\infty M^2}{2}$

α angle of attack, deg

γ ratio of specific heats

MODELS AND TEST APPARATUS

Description of Models

A cross section of the model tested is shown in figure 1 and a photograph is shown in figure 2. Two models of identical profile were built; one was instrumented with pressure orifices whereas the other was adapted to a strain-gage balance. The 10-percent-thick wing had a 5-inch chord and the location of maximum thickness was 3.33 inches (67 percent of chord) from the leading edge. On the lower surface a plate extending from 80 percent of the chord to the trailing edge and to 1/4 inch from each wall was removable, and the base-bleed holes were drilled through this plate. Behind the plate was a hollow chamber which opened into the base of the wing. The wing spanned the 6-inch tunnel except for a clearance of about 0.006 inch at each wall. This clearance permitted balance measurements and changing the angle of attack.

Figure 1 shows the arrangement and spacing of the holes drilled in the lower surface plates. The arrangement of the holes was not exactly the same on the strain-gage model as on the pressure-orifice model. The sketch shows one of the fastening screws which held the plate to the model. On the strain-gage model, these screws interfered with the forwardmost

rows of holes and therefore the area ratio A_H/A_B did not increase lin-
early with the number of rows of holes. On the pressure-orifice model,
this difficulty was avoided by placing all the holes downstream of the
screws. The maximum-area ratios tested were 0.32 on the pressure-orifice
model and 0.444 on the strain-gage model. The diameter of the holes was
0.040 inch.

In figure 2 the strain-gage model is shown mounted between the side
walls but with the nozzle blocks removed. Two identical three-component
balances, one on each side of the model, were attached to the shafts
extending from the model at its point of maximum thickness through the
side walls. On the balance model these holes in the side walls were
clearance holes to prevent fouling and the balances were enclosed in
pressure-tight boxes to minimize leakage of air into the test section.
These pressure boxes have been removed in figure 2. The readings of the
two balances were combined electrically and read as a single output for
each component.

On the pressure model, the shafts on the model were longer and
attached directly to the yoke assembly (see fig. 2). Bushings were
inserted in the holes in the side walls to provide a bearing point and
to minimize air leakage in the absence of the pressure-tight boxes.

An orifice measured the pressure on the forward surface of the hol-
low chamber on the model center line at the midspan (see fig. 1) and this
pressure is called base pressure in this paper. At the completion of the
base-pressure tests, the pressure model was used to check the wing-surface
spanwise pressure distribution near the trailing edge. For this purpose
a row of orifices was made in a plate which did not contain base-bleed
holes. The orifices extended from the model center line to one wall along
a line 1/4 inch from the trailing edge.

Angle-of-Attack and Test Conditions

A motor-powered actuator was attached to the yoke assembly so that
the angle of attack could be changed during a run. The resistance of a
spiral-wound resistor indicated the position of the actuator and thus the
angle of attack. This system had an accuracy of only about $\pm 0.5^{\circ}$; there-
fore, the values of angle of attack in this paper are limited to this
accuracy.

The tests were conducted in the Langley Gas Dynamics Branch in the
small tunnel shown in figure 2. The test section of the tunnel measured
6 by $5\frac{1}{4}$ inches. The free-stream Mach number was 2.72 and the tests were
run at a Reynolds number of 7×10^6 based on the wing chord. The angle
of attack was varied from 0° to 5°.

RESULTS AND DISCUSSION

Figure 3 shows the decrease in the absolute value of the base-pressure coefficient as the area of the holes is increased for the angle-of-attack range, 0° to 5°. The decrease in base-pressure coefficient for the maximum value of A_H/A_B tested on this model was less than the greatest decrease found in reference 3. The slope of the curves indicates some further small gains could be achieved with larger area ratios A_H/A_B. The value of C_{p_B} at zero bleed area checks well with other two-dimensional base-pressure data. For the higher values of A_H/A_B, it appears that the reduction in base-pressure coefficient would be about one-third at an angle of attack of 0° and about one-half at an angle of attack of 5°.

Figure 4 shows the measured angle of attack α plotted against the lift coefficient C_L. The scatter of these data points is believed to be nearly all due to the inaccuracy with which α was measured. The theoretical lift curve as computed by shock-expansion theory is also shown on figure 4. For the remainder of the data C_L is used as the independent variable.

In figure 5 the drag coefficient is plotted against the lift coefficient of the model for various values of A_H/A_B. The data are cross-plotted in figure 6 to show the effect on drag coefficient of varying A_H/A_B at constant values of C_L. It may be seen that increasing the area ratio A_H/A_B near zero lift produces a small but steady decrease in the drag coefficient, but for lift coefficients above 0.075 there is an optimum area ratio. This optimum point becomes more pronounced as the lift coefficient increases.

At zero lift, the decrease in total drag shown in figure 6 is about one-sixth the zero-bleed base drag, as may be seen by converting the base-pressure coefficient of figure 3 to a base drag coefficient. Thus, the maximum base bleed on this model had a net effectiveness of less than 17 percent in eliminating base drag. In figure 3, extrapolation of the zero-lift curve to $A_H/A_B = 0.444$ indicates a corresponding gross reduction in base drag of about 31 percent. Since the base drag is a relatively small part of the total drag, especially as the lift increases, the overall drag reduction (fig. 6) is only about 6 percent at $C_L = 0$ and about 4 percent at $C_L = 0.15$.

In figure 7 the lift-drag ratio C_L/C_D is shown plotted against C_L and in figure 8 the effect on C_L/C_D of varying area ratio is shown

for constant values of C_L. It should be noted that the tests were not carried to high enough angles of attack to show the maximum C_L/C_D of the model. Higher angles of attack could not be tested without exceeding the safe load limit of the balance. However, the maximum C_L/C_D as a function of A_H/A_B at constant C_L was found and figure 8 indicates this peak to be more pronounced with increasing C_L. The influence of base bleed on C_L/C_D at higher values of C_L would be dependent on the condition of upper-surface separation at the trailing edge. Figure 8 shows the net gains for optimum value of A_H/A_B are small and amount to a maximum of 4 percent for $C_L = 0.15$.

Figure 9 indicates that there was practically no change in pitching-moment coefficient with varying area ratio. The theoretical pitching-moment curve is shown in figure 9 and shows good agreement with the data.

In an effort to ascertain roughly the effect of the side-wall boundary layer on the model, measurements were made of the spanwise pressure distribution on the lower surface at a station 1/4 inch from the trailing edge and extending from the model center line to within 1/4 inch of the wall. These results are presented in figure 10. It may be seen that the pressure is lower near the wall than in the center portion and that the region near the wall is affected by the presence of the tunnel side wall. This gradient is imposed by the changes in thickness of the side-wall boundary layer which has in turn been influenced by the presence of the model. The results indicate the gradient is not greatly affected by changes in angle of attack although the gradient near the wall steepens somewhat. Also shown in figure 10 is the pressure distribution at an angle of attack of 0° when the small clearance gap between the model and the side wall has been filled in. The difference between the general level of the two curves is attributed to the uncertainty with which the angle of attack is set. Comparison of the two curves at $\alpha = 0$, with the gap filled and unfilled, indicates that flow around the ends of the model through the gap is not the primary cause of the spanwise pressure gradient. The data cannot be interpreted as truly two dimensional because of this spanwise gradient. It is felt, however, that the trends of the data are indicative of those on a true two-dimensional model and that the gradient does not seriously affect the validity of the data.

CONCLUDING REMARKS

A 10-percent-thick blunt-base airfoil section was tested at a Mach number of 2.72 to determine the effects of base bleed on base pressure,

lift, drag, and pitching moment. The base bleed was accomplished on this model by perforating the lower surface of the wing near the trailing edge with small holes. Thus, air was drawn off the lower surface into the base region by the existing pressure differential. The tests were conducted for the angle-of-attack range $0°$ to $5°$ and for various total areas of the bleed holes up to 44 percent of the base area.

Results of the tests on this model indicated the base drag could be reduced by about one-third at an angle of attack of $0°$ and by one-half at an angle of attack of $5°$. However, the penalty that must be paid for this reduction in base drag is a drag increase due to the bleed-air-induction system. On the model tested, small or even negligible net gains were realized because this drag penalty was of the same order as the base-drag decrease. The zero-lift drag coefficient was reduced about 6 percent but at a lift coefficient of 0.15 the greatest drag reduction was about 4 percent.

Langley Aeronautical Laboratory,
        National Advisory Committee for Aeronautics,
                Langley Field, Va., October 25, 1954.

REFERENCES

1. Chapman, Dean R.: Airfoil Profiles for Minimum Pressure Drag at Supersonic Velocities - Application of Shock-Expansion Theory, Including Consideration of Hypersonic Range. NACA TN 2787, 1952.

2. Cortright, Edgar M., Jr., and Schroeder, Albert H.: Preliminary Investigation of Effectiveness of Base Bleed in Reducing Drag of Blunt-Base Bodies in Supersonic Stream NACA RM E51A26, 1951.

3. Wimbrow, William R.: Effects of Base Bleed on the Base Pressure of Blunt-Trailing-Edge Airfoils at Supersonic Speeds. NACA RM A54A07, 1954.
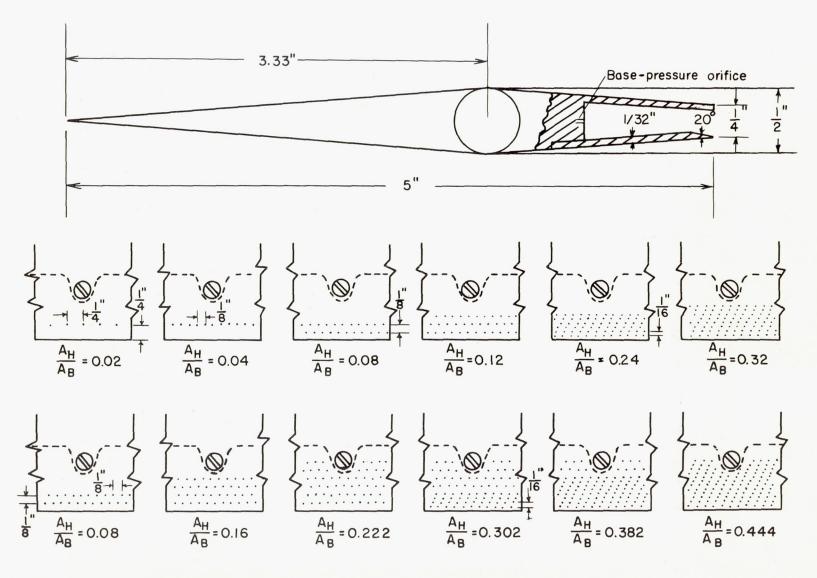
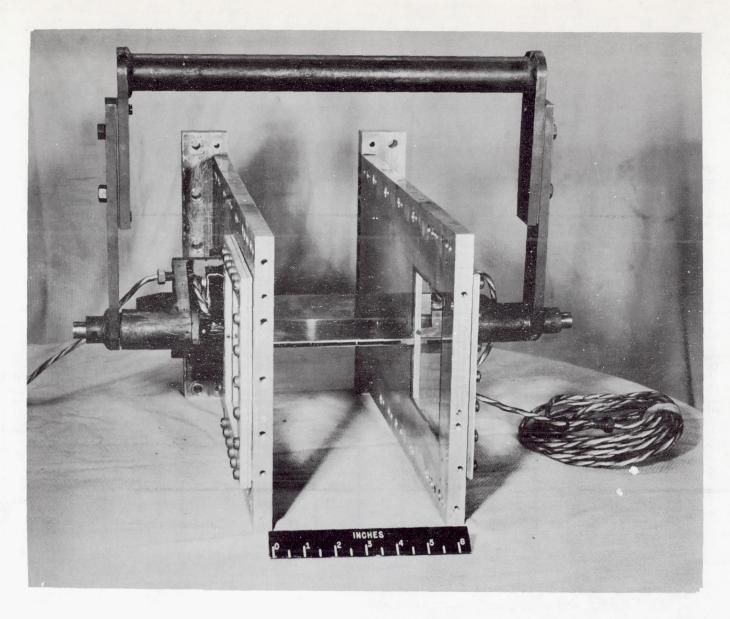Figure 1.- Sketch of model tested and arrangement of base-bleed holes.

Figure 2.- Photograph of strain-gage model mounted between sidewalls. L-85340
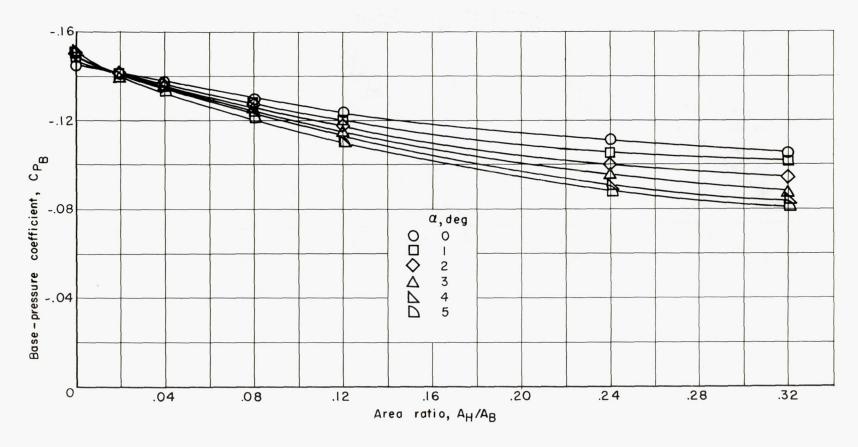
Figure 3.- Variation of base pressure with area ratio for angle-of-attack range tested.
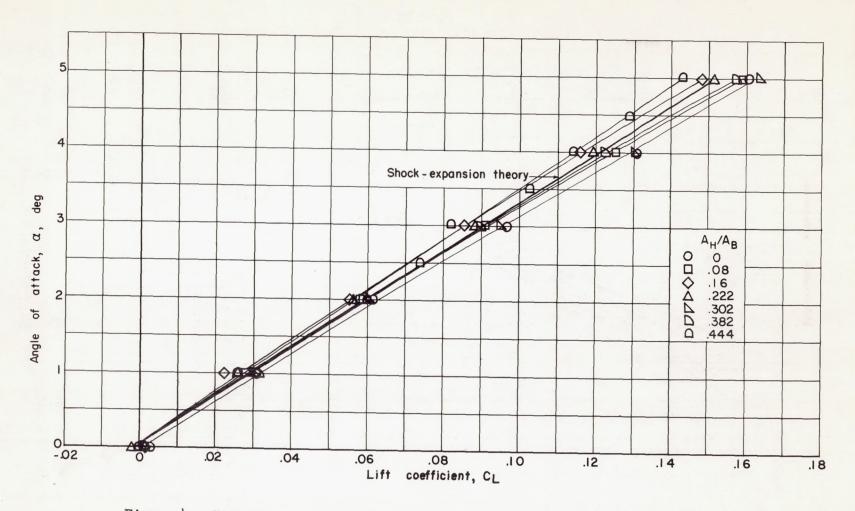
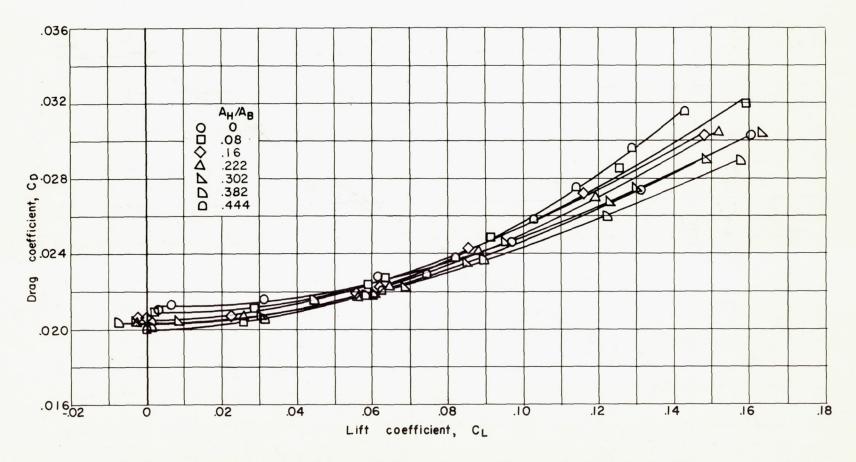Figure 4.- Variation of measured angle of attack with lift coefficient.

Figure 5.- Variation of drag coefficient with lift coefficient for various area ratios.
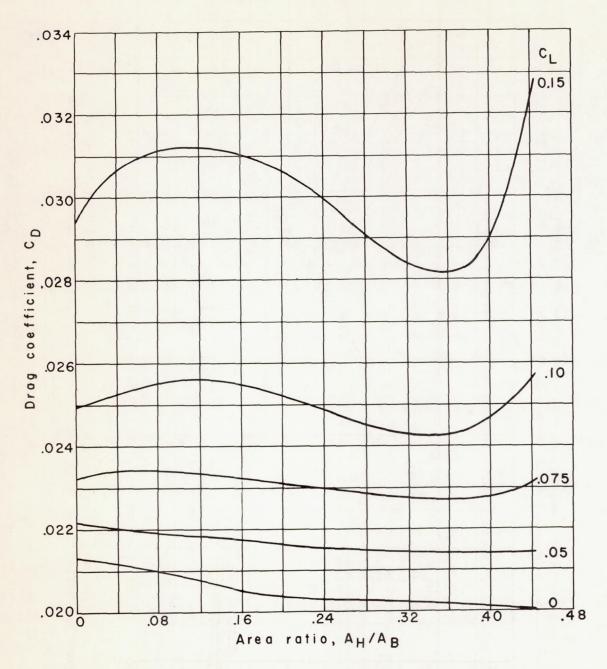
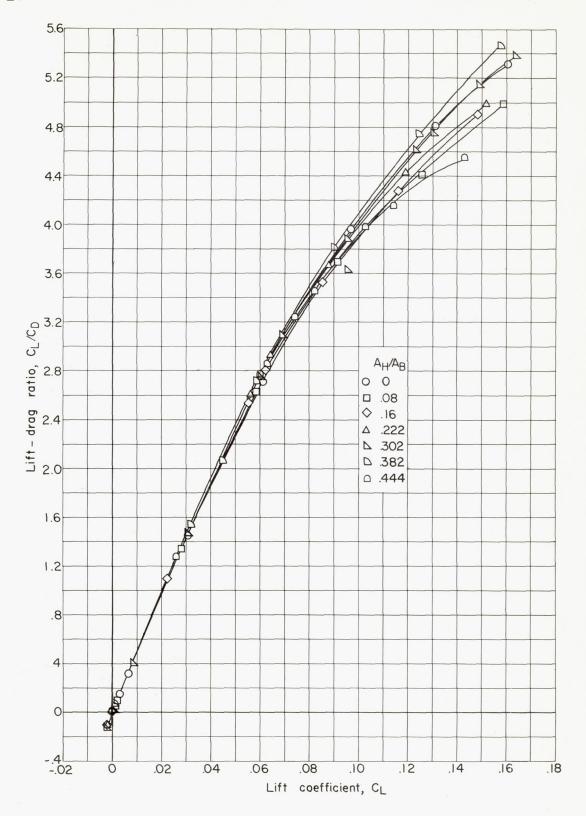Figure 6.- Variation of drag coefficient with area ratio for various lift coefficients.

Figure 7.- Variation of lift-drag ratio with lift coefficient for various
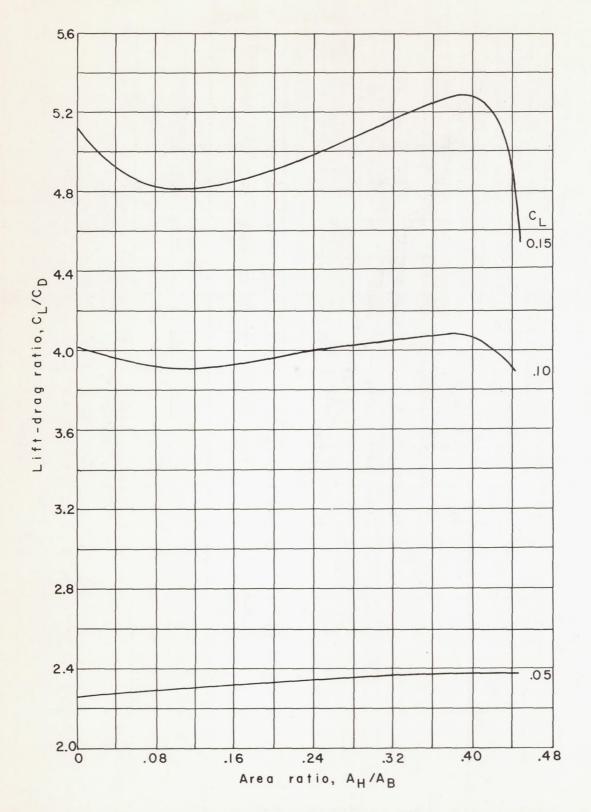area ratios.

Figure 8.- Variation of lift-drag ratio with area ratio for various lift coefficients.
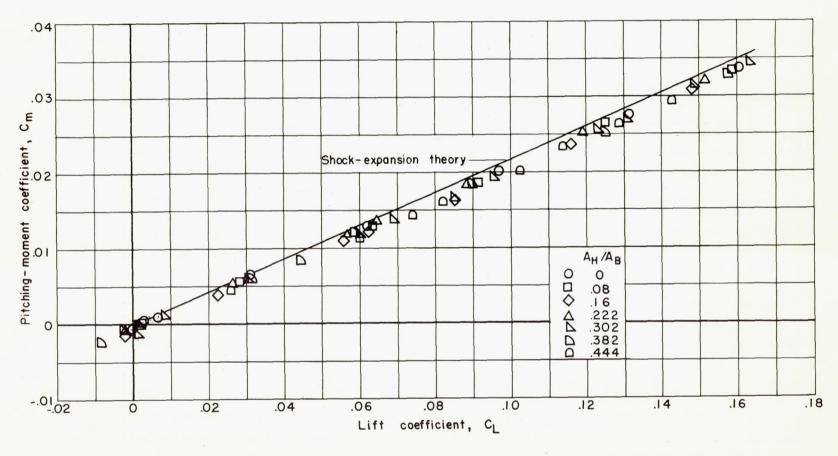
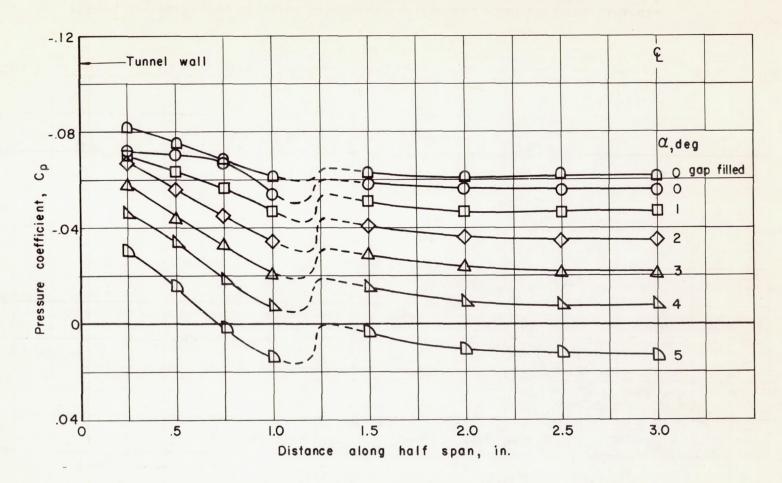Figure 9.- Variation of pitching-moment coefficient with lift coefficient.

Figure 10.- Variation of pressure coefficient on lower surface 0.25 inch
ahead of trailing edge.